Kinetics of the Cis,Cis to Trans,Trans Isomerization of 1,1,2,2,5,5,6,6-Octamethyl-1,2,5,6-tetrasilacycloocta-3,7-diene

Lei Zhang, Christopher W. Borysenko,*,† and T. Randall Lee*

Department of Chemistry, University of Houston, Houston, Texas 77204-5003

trlee@uh.edu

Received October 16, 2000 (Revised Manuscript Received June 7, 2001)

The kinetics of the ruthenium-promoted cis,cis to trans,trans isomerization of 1,1,2,2,5,5,6,6-octamethyl-1,2,5,6-tetrasilacycloocta-3,7-diene were investigated. Incubation of a ruthenium alkylidene complex, $(Cy_3P)RuCl_2(=CHPh)Ru(p\text{-cymene})Cl_2$, in CD_2Cl_2 for 5 days at 40 °C afforded a catalytically active ruthenium species that was shown to be responsible for promoting the isomerization. The isomerization was observed to proceed in two steps: (1) conversion of the starting cis,cis isomer to a proposed cis,trans intermediate and (2) subsequent conversion of the intermediate to the product trans,trans isomer. Kinetic studies demonstrated that the two steps are first-order with respect to the concentrations of the cis,cis isomer, the intermediate, and the ruthenium alkylidene complex. The data were further consistent with a mechanism involving bimolecular hydride addition−elimination during the two isomerization steps.

Introduction

In the presence of transition-metal catalysts, a commonly observed pathway for the cis−trans isomerization of 1,2-disubstituted olefins involves the stepwise addition/elimination of a metal hydride to the carbon−carbon double bond of the olefin (Scheme 1).[1−3] In these reactions, free olefin coordinates to a kinetically long-lived metal hydride species and subsequently inserts into the metal−hydride bond to yield a metal alkyl and a new C−H bond. Productive β-elimination of the original C−H bond yields the cis−trans isomerized olefin and regenerates the metal hydride. While many of the transition-metal complexes that catalyze this reaction exist as stable, isolable metal hydrides (e.g., $HCo(CO)_4$, $RhH(CO)(PPh_3)_3$, $IrH(CO)(PPh_3)_3$, and $RuHCl(PPh_3)_3$), many do not (e.g., $RhCl_3$, $RhCl(PPh_3)_3$, $Ni(P(OEt)_3)_4$). The latter systems require acids[4−7] and hydrogen[8,9] as cocatalysts, which serve to generate the active metal hydride species.

Recently developed ruthenium alkylidene complexes described by Grubbs and co-workers[10,11] can be used to promote the ring-opening metathesis polymerization (ROMP) of strained cyclic olefins.[12−15] During, however, the course of our attempted ROMP of *cis,cis*-1,1,2,2,5,5,6,6-octamethyl-1,2,5,6-tetrasilacycloocta-3,7-diene (**1a**) by exposure to the dimeric ruthenium(II) alkylidene complex $(Cy_3P)RuCl_2(=CHPh)Ru(p\text{-cymene})Cl_2$ (**Ru**),[10] we surprisingly discovered that, in contrast to ROMP, the ruthenium complex served to catalyze the cis,cis to trans,-trans isomerization of the double bonds of **1a** to give *trans,trans*-1,1,2,2,5,5,6,6-octamethyl-1,2,5,6-tetrasilacycloocta-3,7-diene (**1b**) (eq 1).[16] As a complement to the preceding mechanistic analysis of the isomerization of **1a** to **1b** in which the reaction pathway is indicated to proceed via metal hydride addition/elimination,[17] we report here the kinetic features of this unique isomerization and demonstrate that the kinetic profiles provide further support for the proposed mechanism of isomerization.

Scheme 1

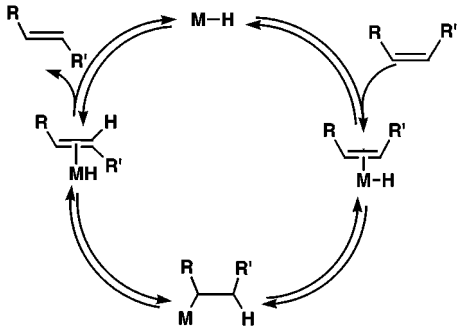

* To whom correspondence should be addressed. E-mail: borysenkocw@msx.upmc.edu and trlee@uh.edu.

† Pittsburgh Cancer Institute, W1011 Biomedical Science Tower, 200 Lothrop Street, Pittsburgh, PA 15213.

(1) Parshall, G. W. *Homogeneous Catalysis*; Wiley: New York, 1980; pp 31−35.

(2) Crabtree, R. H. *The Organometallic Chemistry of the Transition Metals*; Wiley: New York, 1988; pp 188−190.

(3) McGrath, D. V.; Grubbs, R. H. *Organometallics* **1994**, *13*, 224.

(4) Cramer, R. *J. Am. Chem. Soc.* **1966**, *88*, 2272.

(5) Cramer, R.; Lindsey, R. V., Jr. *J. Am. Chem. Soc.* **1966**, *88*, 3534.

(6) Tolman, C. A. *J. Am. Chem. Soc.* **1972**, *94*, 2994.

(7) Cramer, R. *Acc. Chem. Res.* **1968**, *1*, 186.

(8) Adams, R. W.; Batley, G. E.; Bailar, J. C., Jr. *J. Am. Chem. Soc.* **1968**, *90*, 6051.

(9) Baudry, D.; Ephritikihne, M.; Felkin, H. *J. Chem. Soc., Chem. Commun.* **1978**, 694.

(10) Dias, E. L.; Grubbs, R. H. *Organometallics* **1998**, *17*, 2758.

(11) Miller, S. J.; Kim, S. H.; Chen, Z.; Grubbs, R. H. *J. Am. Chem. Soc.* **1995**, *117*, 2108.

(12) Grubbs, R. H.; Tumas, W. *Science* **1989**, *243*, 907.

(13) Dragutan, V.; Balaban, A. T.; Dimonie, M. *Olefin Metathesis and Ring-Opening Polymerization of Cyclo-Olefins*; Wiley: New York, 1985; p 544.

(14) Ivin, K. J. *Olefin Metathesis*; Academic: London, 1983.

(15) Grubbs, R. H.; In *Comprehensive Organometallic Chemistry*; Wilkinson, G., Ed.; Pergamon Press: New York, 1982; Vol. 8, pp 499−551.

(16) Zhang, L.; Jung, D.-Y.; Bittner, E. R.; Sommer, M. S.; Dias, E. L.; Lee, T. R. *J. Org. Chem.* **1998**, *63*, 8624.

(17) Zhang, L.; Borysenko, C. W.; Albright, T. A.; Bittner, E. R.; Lee, T. R. *J. Org. Chem.* **2001**, *66*, 5275.

10.1021/jo0014820 CCC: $20.00
Published on Web 07/13/2001

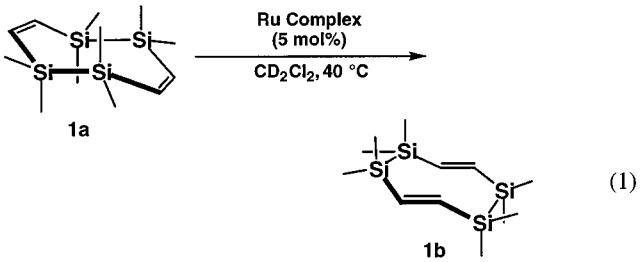

(1)

Results and Discussion

Kinetics: General Approach. The synthesis of **1a** and a preliminary investigation of its ruthenium-catalyzed isomerization to **1b** have been reported.[16] As shown in eq 1, exposure of **1a** to a catalytic amount of **Ru** in CD_2Cl_2 at 40 °C affords **1b**. We explored the kinetics of the isomerization by varying the concentration of **1a** and **Ru** and by monitoring the progress of the reaction using ^{1}H NMR spectroscopy.

Kinetics Methods. The progress of the isomerization of a 13−80-fold molar excess of **1a** to **Ru** was monitored in a Schlenk NMR tube by examining the ^{1}H NMR spectroscopic resonances (see Figure 1) for the disappearance of the cis-olefinic protons (δ 6.90), the appearance of the trans-olefinic protons (δ 6.32), the appearance of two singlets (δ 6.78 and 6.88), which we assign to the formation of an intermediate designated **1i**, and the appearance of two singlets (δ 6.94 and 6.98), which we assign to a derivative of **Ru** designated **Ru′**; the basis for the latter two assignments will be described in detail in a later section. In Figure 1, we assign the broad resonance at δ 6.32 ppm to the protons of **1b** by comparison to the spectrum of authentic, crystalline material.[16−18] The two singlets corresponding to **1i** are consistent with a tenable cis,trans intermediate (vide infra).

Due to the nature of the kinetic profiles and the presence of overlapping resonances in the ^{1}H NMR spectra (see Figure 1), we performed the integration and evaluation of the isomerization kinetics in the following manner. For the initial loss of **1a**, the peaks corresponding to **1i** at δ 6.78 and 6.88 appeared first (integrating roughly 1:1). Subsequently, the peaks corresponding to **Ru′** at δ 6.94 and 6.98 (integrating roughly 1:1) and the peak corresponding to **1b** at δ 6.32 appeared; the defining characteristics of these "initial loss" and the "steady-state" kinetic regimes will be described in a later section. To quantify **1a** in the "initial loss" regime, we integrated over the range δ 6.85−7.05 and subtracted from this integral the area of the isolated peak at δ 6.78, which approximates the area of the overlapped peak at δ 6.88. To quantify **1a** in the "steady-state" regime, however, we used a different method due to the presence of the **Ru′** resonances at δ 6.94 and 6.98. Since, in this regime, all four small peaks at δ 6.78, 6.88, 6.94, and 6.98 exhibit roughly the same peak heights, we integrated over the range δ 6.85−7.05 and subtracted three times the area of the isolated peak at δ 6.78 (this area approximates that of the three overlapped peaks at δ 6.88, 6.94, and 6.98). All integrals were referenced internally to a known quantity of ferrocene at δ 4.18.

Prior to the addition of **1a**, the Schlenk NMR tubes were charged with **Ru,** ferrocene (as an internal standard), and CD_2Cl_2 and then held at 40 °C for 5 days. This pretreatment of the complex was found to eliminate a lag in the consumption of **1a**, which was observed when **1a** was included in the reaction mixture at the start of the incubation (see Figure 2). Similar induction periods for the activation of metal hydride isomerization catalysts have been reported.[19] In these studies, the activation processes are believed to involve the reaction of the ruthenium precursors with trace acid in the solvent to generate catalytically active ruthenium hydride species.

To further address the nature of the observed lag, we explored the use of other ruthenium hydride sources to effect the isomerization of **1a** to **1b**. Exposure, for example, of **1a** to the commercially available ruthenium(II) hydride complex chlorohydridotris(triphenylphosphine)-ruthenium(II) ($(Ph_3P)_3Ru(Cl)H$) and dihydridotetrakis(triphenylphosphine)ruthenium(II) ($(Ph_3P)_4RuH_2$) in CD_2Cl_2 at 40 °C also afforded isomer **1b**.[16,17] We also found that dichloro(*p*-cymene)ruthenium(II) dimer [Ru(*p*-cymene)-

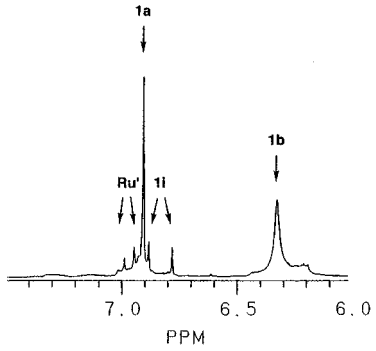

Figure 1. Selected region of the 300 MHz ^{1}H NMR spectrum of the conversion of **1a** to **1b**. The reaction of 0.351 M **1a** in CD_2Cl_2 at 40 °C was observed at 96 h after the addition of 0.0088 M **Ru**. The peak assignments of the olefinic protons are as follows: **1a**, 6.90 ppm; **1b**, 6.32 ppm; **1i**, 6.78 and 6.88 ppm. The peaks at 6.94 and 6.98 ppm are assigned to the catalyst (see text).

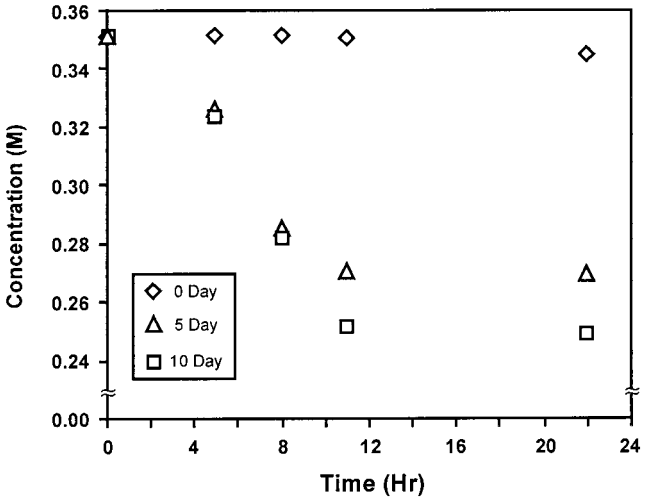

Figure 2. Isomerization of 0.35 M **1a** in CD_2Cl_2 at 40 °C catalyzed by 0.0088 M **Ru**. The catalyst was preincubated in the solvent for 0 (diamonds), 5 (triangles), and 10 days (squares) prior to the addition **1a**. The relative invariance of the data in the absence of preincubation is characteristic of the induction period.

(18) The broad peak centered near δ 6.32 arises from the occupancy of two low-energy conformers of **1b** as described in ref 17.

(19) Patil, S. R.; Sen, D. N.; Chaudhari, R. V. *J. Mol. Catal.* **1984**, *23*, 51.

$Cl_2]_2$ catalyzed the isomerization, but at rates at least 1 order of magnitude slower than that of all other Ru-based catalysts. Moreover, bis(cyclopentadienyl)zirconium(II) chloride hydride ($Cp_2Zr(Cl)H$) also effected the isomerization, but at rates substantially slower than that of the Ru-based catalysts. All catalysts displayed induction periods analogous to that displayed by **Ru**. The duration of the induction period, however, varied according to nature of the catalyst employed: $Cp_2Zr(Cl)H$ > (Ru(*p*-cymene)$Cl_2)_2$ > $(Ph_3P)_4RuH_2$ > $(Ph_3P)_3Ru(Cl)H$) > **Ru**. The overall rates of isomerization of **1a** to **1b** mirrored the reverse of the induction period trend: **Ru** > $(Ph_3P)_3$-Ru(Cl)H) > $(Ph_3P)_4RuH_2$ > (Ru(*p*-cymene)$Cl_2)_2$ > Cp_2Zr-(Cl)H. Due to the remarkably slow isomerization of **1a** to **1b** at 40 °C, the instability of **1b** at elevated temperatures, and the fact that the isomerization proceeded most rapidly when using **Ru** as the catalyst precursor, we chose to use **Ru** as the catalyst precursor for the kinetic studies described herein.

As noted above for reactions promoted by **Ru**, four small singlets in the olefinic region were observed during the course of the isomerization (δ 6.78, 6.88, 6.94, and 6.98) in addition to those of **1a** (δ 6.90) and **1b** (δ 6.32). For all other catalysts, however, only the two small singlets at δ 6.78 and 6.88 were observed; the other two at δ 6.94 and 6.98 were absent. Moreover, the area of the singlets at δ 6.78 and 6.88 were indistinguishable. On the basis of these observations and an analysis of the 600 MHz ^{1}H NMR COSY spectra of the intermediates, which shows that none of the singlets are coupled (data not shown), we assign the singlets at δ 6.78 and 6.88 to a C_2-symmetric conformation of the cis,trans intermediate **1i** (eq 2).[19] Moreover, due to our detection of the

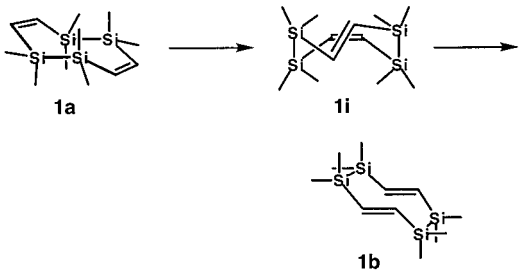

(2)

singlets at δ 6.94 and 6.98 in only the isomerizations catalyzed by **Ru**, we propose that these singlets arise from **Ru** itself. We admit, however, that **Ru** might somehow effect the partial decomposition of **1a** (or of a derivative of **1a**) that gives rise to these singlets. We do not account for the latter possibilities in the analyses presented here.

Progress Curves for the Isomerization of 1a. The isomerization of **1a** was followed over time as a function of the initial concentration of **1a** at a constant **Ru** concentration and as a function of the concentration of the complex in order to determine the order of the reaction with respect to the components. Representative progress curves for the isomerization of 0.351 M **1a** in the presence of 0.0088 M **Ru** are shown in Figure 3 and can be analyzed qualitatively to yield general aspects of the isomerization of **1a** to **1b**. The loss of **1a** is biphasic; the initial rate of loss of the cis,cis isomer diminishes over time. There is a lag in the formation of **1b**, which coincides with the onset of the slower rate of loss of **1a**. The initially faster rate of loss of **1a**, during which time

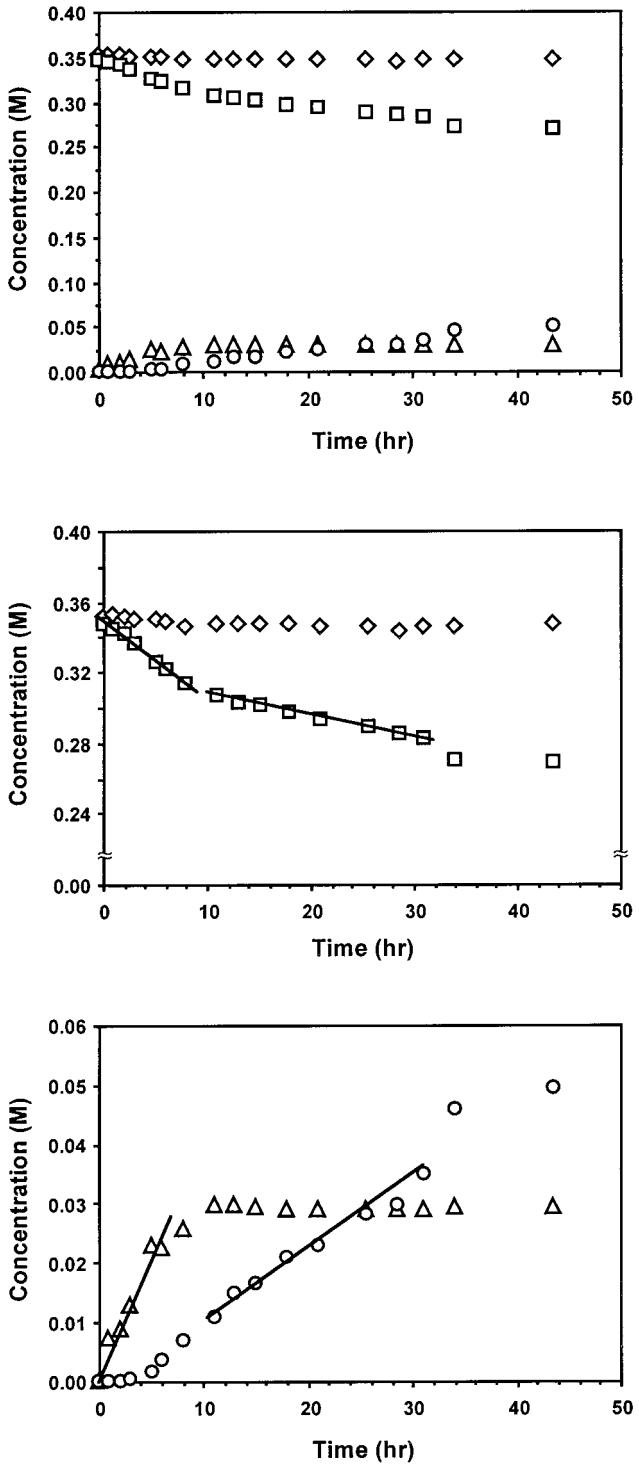

Figure 3. (Top) Representative progress curves of the isomerization of **1a** (squares) into **1i** (triangles) and **1b** (circles) in CD_2Cl_2 at 40 °C in the presence of 0.0088 M **Ru** and initial concentration of **1a** of 0.351 M. The diamond symbols indicate the sum of the concentrations of **1a**, **1i,** and **1b** at each time interval. (Middle and bottom) Selective magnification of portions of the data in the top panel. The lines drawn in the middle and bottom panels illustrate the regions of the progress curves used to calculate the initial and steady-state rates.

1b has yet to form, is accompanied by the formation of an additional species, designated **1i**. The formation of **1i** is also biphasic; its rate of formation diminishes to zero as its concentration becomes time independent. The leveling off of **1i** coincides with the formation of **1b** and

Table 1. Observed Steady-State Concentration of 1i ($[1i]_{ss}$, M), the Initial Rates ($\times 10^3$, M/h) of Loss of 1a ($R_{1a,i}$) and Formation of 1i ($R_{1i,i}$), and the Steady-State Rate ($\times 10^3$, M/h) of Loss of 1a ($R_{1a,ss}$) and Formation of 1b ($R_{1b,ss}$)[a]

$[\mathbf{Ru}]_0$ (M)	$[\mathbf{1a}]_0$ (M)	$[\mathbf{1i}]_{ss}$	$R_{\mathbf{1a},i}$	$R_{\mathbf{1i},i}$	$R_{\mathbf{1a},ss}$	$R_{\mathbf{1b},ss}$
0.0088	0.044	0.006	0.43	0.43	0.21	0.15
0.0088	0.088	0.008	0.81	0.81	0.29	0.34
0.0088	0.176	0.017	1.65	1.65	0.63	0.58
0.0088	0.351	0.030	3.60	3.60	1.21	1.18
0.0022	0.176	0.017	0.41	0.41	0.21	0.10
0.0044	0.176	0.014	0.78	0.78	0.36	0.18
0.0088	0.176	0.016	1.65	1.65	0.63	0.60
0.0132	0.176	0.016	2.26	2.26	1.02	1.14

[a] The values of $R_{\mathbf{1i},i}$ are measured as the slopes of the lines tangent to the initial phase of **1i** formation. The values of $R_{\mathbf{1a},i}$ are calculated on the basis of $R_{\mathbf{1i},i}$. The values of $R_{\mathbf{1a},ss}$ and $R_{\mathbf{1b},ss}$ are measured as the slopes of the progress curves in the steady-state region (see Figure 3).

the slower rate of loss of **1a**. These features of the progress curves are consistent with an initial pre-steady-state phase, which encompasses the lag in the production of **1b**, and a steady-state phase in which the concentration of **1i** is time invariant.

Figure 3 further demonstrates that the sum of the concentrations of **1a**, **1i**, and **1b** over the course of the isomerization maintains a constant value equal to the initial concentration of **1a** (note the invariance of concentration values denoted by the diamond symbols as function of time). These data are consistent with a model in which the cis,cis isomer is converted into the trans,-trans isomer and **1i** without forming appreciable quantities of other unidentified species.

The lag in the formation of **1b** in Figure 3 is consistent with the intermediate **1i** lying on the pathway for the conversion of **1a** into **1b**. Another possibility is that **1i** and **1b** are both formed directly from **1a** and that **1i** is not a precursor to **1b**. However, the lag in the formation of **1b**, concomitant with the formation of **1i**, suggests that **1a** is first converted into **1i**; therefore, the concentration of **1a** is lower during the steady-state period than its initial concentration. If **1b** were to form directly from **1a**, then the rate of formation of **1b** would be greater in the pre-steady-state period and diminished during the steady state as dictated by the reduced level of **1a** in the steady state. Thus, the direct formation of **1i** and **1b** from **1a** predicts a burst in the formation of **1b** and not the observed lag. We thus conclude that **1i** is an intermediate on the pathway for the conversion of **1a** into **1b**.

Rates from the Progress Curves of the Isomerization of 1a. Values for the initial rates of loss of **1a** ($R_{\mathbf{1a},i}$) and formation of **1i** ($R_{\mathbf{1i},i}$) as a function of the concentrations of **1a** and **Ru** were obtained from progress curves similar to those in Figure 3 by measuring the tangents to the curves in the initial pre-steady-state regime of the isomerizations. The steady-state rates of loss of **1a** ($R_{\mathbf{1a},ss}$) and the steady-state rates of formation of **1b** ($R_{\mathbf{1b},ss}$) were calculated as the slopes of the progress curves in this region of the reactions and the resulting values of the calculated rates and the values of the observed steady-state concentrations of **1i** are listed in Table 1. The values of the observed rates are plotted in Figures 4 and 5 as a function of the concentration of the varied component of the reaction. The initial rate of loss of **1a,** the steady-state rate of loss of **1a**, and the steady-state rate of formation of **1b** are linear functions of the concentrations of **1a** and **Ru**. The linearity indicates that

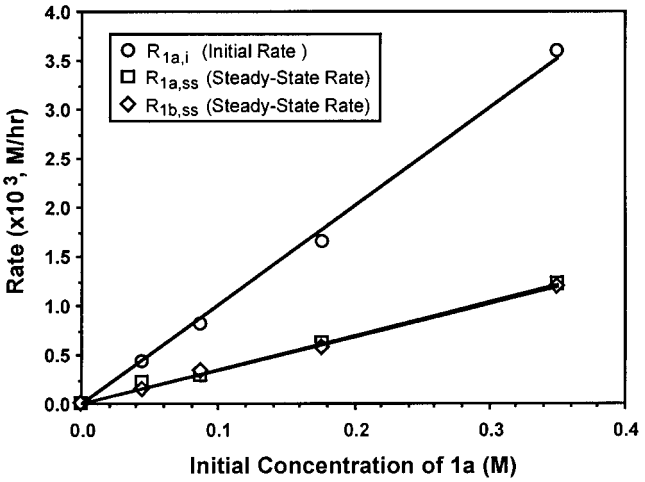

Figure 4. Initial rates of the loss of **1a** (circles, $R_{\mathbf{1a},i}$), the steady-state rates of loss of **1a** (squares, $R_{\mathbf{1a},ss}$), and the steady-state rates of formation of **1b** (diamonds, $R_{\mathbf{1b},ss}$) as a function of the initial concentration of **1a** (0.044, 0.088, 0.176, and 0.351 M) in the presence of 0.0088 M **Ru** in CD_2Cl_2 at 40 °C. The observed slope for the initial rate data is 0.010 h^{-1}, which, according to eq 5, equals the pseudo-first-order rate constant for the conversion of **1a** to **1i** and corresponds to the second-order rate constant of 1.1 M^{-1} h^{-1}. The observed slopes for the steady-state data are both 0.0034 h^{-1}; the predicted values of the slopes, according to eq S8 (see the Supporting Information) and the observed second-order rate constants from Table 2, are both 0.0034 h^{-1}.

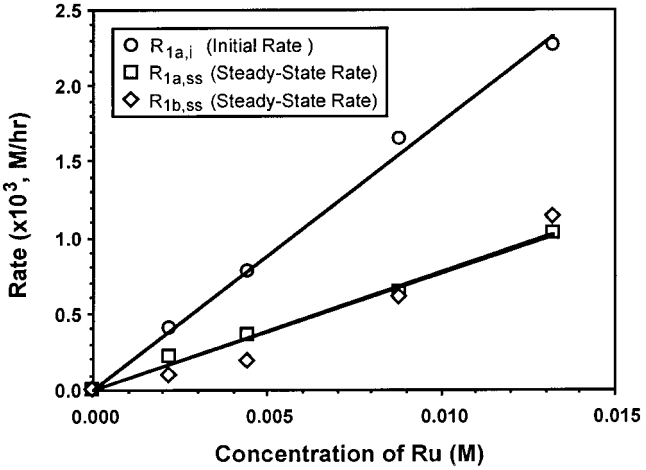

Figure 5. Initial rates of the loss of 0.176 M **1a** (circles, $R_{\mathbf{1a},i}$), the steady-state rates of loss of **1a** (squares, $R_{\mathbf{1a},ss}$), and the steady-state rates of formation of **1b** (diamonds, $R_{\mathbf{1b},ss}$) as a function of the total concentration of **Ru** (0.0022, 0.0044, 0.0088, and 0.0132 M) in CD_2Cl_2 at 40 °C. The observed slope for the initial rate data is 0.18 h^{-1}, which, according to eq 5, equals the pseudo-first-order rate constant for the conversion of **1a** to **1i** and corresponds to the second-order rate constant of 1.0 M^{-1} h^{-1}. The observed slopes for the steady-state data are both 0.077 h^{-1}; the predicted values of the slopes, according to eq S8 (see the Supporting Information) and the observed second-order rate constants from Table 2, are both 0.069 h^{-1}.

both the conversion of the cis,cis isomer into intermediate **1i**, and the conversion of **1i** into the trans,trans isomer **1b**, are first order with respect to **1a** and first order with respect to **Ru**. Moreover, the observed steady-state concentrations of **1i** in Table 1 are independent of the concentration of **Ru**, further supporting the role of the catalyst in both steps of the reaction.

The linearity of the data in Figures 4 and 5 also indicates that, at the concentrations used, the catalyst is not saturated with starting material; otherwise, the reaction would be zero order with respect to **1a**. This result is similar to the pseudo first-order kinetics observed for the ROMP of 1,5-cyclooctadiene by **Ru**,[10] and is also consistent with the pseudo first-order kinetics observed for olefin isomerizations catalyzed by $(PPh_3)_3$-Ru(Cl)H.[20]

Pseudo-First Order and Second-Order Rate Constants for the Isomerization of 1a. The above qualitative analysis of the rates of isomerization of **1a** as a function of the concentrations of **1a** and **Ru** is consistent with the second-order conversion of **1a** into **1i** and the second-order conversion of **1i** into **1b**. Each step is first order in starting material and in **Ru**. A more detailed analysis of the rates allows the calculation of rate constants for each phase of the reaction. The minimal representation of the kinetics of the isomerization reaction is provided in eqs 3 and 4.[14,15]

$$\mathbf{1a} + \mathbf{Ru} \underset{k_{-1}}{\overset{k_1}{\rightleftharpoons}} \mathbf{1a\text{-}Ru} \underset{k_{-2}}{\overset{k_2}{\rightleftharpoons}} \mathbf{1i} + \mathbf{Ru} \qquad (3)$$

$$\mathbf{1i} + \mathbf{Ru} \underset{k_{-3}}{\overset{k_3}{\rightleftharpoons}} \mathbf{1i\text{-}Ru} \xrightarrow{k_4} \mathbf{1b} + \mathbf{Ru} \qquad (4)$$

In the first step (eq 3), **1a** binds to the catalyst and then reacts and dissociates to afford **1i** and the catalyst. In this model, all steps in phase one are reversible in order to account for the smaller steady-state rate of loss of **1a** ($R_{\mathbf{1a},ss}$) compared to the initial rate of loss of **1a** ($R_{\mathbf{1a},i}$) (see Table 1 and the discussion below). In the second phase of the reaction (eq 4), **1i** binds to the catalyst and then reacts and dissociates to afford **1b** and the catalyst. In this phase of the reaction, the second step, with rate constant k_4, is considered to be effectively irreversible (that is, k_{-4} is zero) in order to allow the mathematical treatment to be tractable. This assumption is, however, valid since we have observed that neither **1i** nor **1a** form upon the incubation of purified **1b** with **Ru**,[16,17] suggesting that the overall reaction has a large equilibrium constant.

Under the conditions of the present study, an expression for the initial rate of loss of **1a**, $R_{\mathbf{1a},i}$, is given by equation 5, where $K_{m1} = (k_2 + k_{-1})/k_1$ (see the Supporting Information), and predicts that the initial rate of loss of **1a** will be first order with respect to both **1a** and **Ru**.[21,22] The linear relationships in Figures 4 and 5 indicate that the assumptions leading to eq 5 are appropriate and that the values of the slopes give the pseudo-first-order rate constants. The second-order rate constants for the initial rate of loss of **1a** are obtained by dividing the pseudo-first-order rate constants by the concentration of the species that was held constant. These values are provided in Table 2 and indicate a good agreement for the second-order rate constants of $k_2/K_{m1} = 1.1$ and 1.0 M^{-1} h^{-1} for the conversion of **1a** into **1i**.

$$R_{\mathbf{1a},i} = \frac{k_2[\mathbf{Ru}]_0[\mathbf{1a}]_0}{K_{m1}} \qquad (5)$$

Table 2. Pseudo-First-Order Rate Constants (h^{-1}) and the Second-Order Rate Constants (M^{-1} h^{-1}) for the Ru-Catalyzed Conversion of 1a to 1i and 1i to 1b[a]

	experimental conditions	
	vary $[\mathbf{1a}]_0$, $[\mathbf{Ru}]_0 = 0.0088$ M	vary $[\mathbf{Ru}]_0$, $[\mathbf{1a}]_0 = 0.176$ M, $[\mathbf{1i}]_{ss} = 0.016$ M
initial loss of **1a**	$k_2[\mathbf{Ru}]_0/K_{m1} = 0.010$ h^{-1} [a]; $k_2/K_{m1} = 1.1$ M^{-1} h^{-1}	$k_2[\mathbf{1a}]_0/K_{m1} = 0.18$ h^{-1} [b]; $k_2/K_{m1} = 1.0$ $M^{-1}h^{-1}$
steady state formation of **1b**	$k_4[\mathbf{Ru}]_0/K_{m2} = 0.038$ h^{-1} [c]; $k_4/K_{m2} = 4.3$ M^{-1} h^{-1}	$k_4[\mathbf{1i}]_{ss}/K_{m2} = 0.077$ h^{-1} [d]; $k_4/K_{m2} = 4.8$ M^{-1} h^{-1}
steady state loss of **1a**	$k_{-1}[\mathbf{Ru}]_0/K_{m-1} = 0.073$ h^{-1} [e]; $k_{-1}/K_{m-1} = 8.3$ M^{-1} h^{-1}	$k_{-1}[\mathbf{1i}]_{ss}/K_{m-1} = 0.10$ h^{-1} [f]; $k_{-1}/K_{m-1} = 6.3$ M^{-1} h^{-1}

[a] The values were obtained from the following: (a) Figure 4, eq 5; (b) Figure 5, eq 5; (c) Figure 6, eq 6; (d) Figure 5, eq 6; (e) Figure S1, eq S5; (f) Figure S2, eq S5.

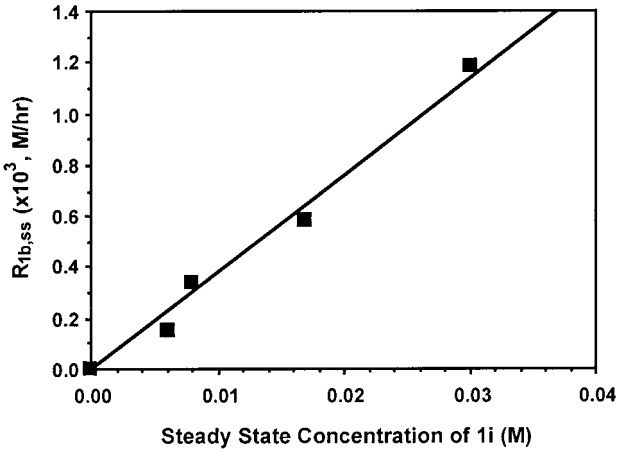

Figure 6. Steady-state rate of formation of **1b** ($R_{\mathbf{1b},ss}$) as a function of the observed steady-state concentrations of **1i** ($[\mathbf{1i}]_{ss}$) in CD_2Cl_2 at 40 °C. The initial concentrations of **1a** were 0.044, 0.088, 0.176, and 0.351 M, and the **Ru** concentration was 0.0088 M. The observed slope is 0.038 h^{-1}, which, according to eq 6, equals the pseudo-first-order rate constant for the conversion of **1i** to **1b** and corresponds to the second-order rate constant of 4.3 M^{-1} h^{-1}.

The steady-state rate of formation of **1b** from **1i**, $R_{\mathbf{1b},ss}$, is given by eq 6, where $K_{m2} = (k_4 + k_{-3})/k_3$ (see the Supporting Information) and predicts that $R_{\mathbf{1b},ss}$ will be first order in $[\mathbf{1i}]_{ss}$ and in $[\mathbf{Ru}]$. The slopes of the steady-state data in Figures 5 and 6 give the values of the pseudo-first-order rate constants and the resulting second-order rate constants of $k_4/K_{m2} = 4.3$ and 4.8 M^{-1} h^{-1} for the conversion of **1i** into **1b** (Table 2). The values of the second-order rate constants, obtained from experiments in which each of the components of the reaction were varied, are in agreement, validating both the model and the analytical approach.

$$R_{\mathbf{1b},ss} = \frac{k_4[\mathbf{Ru}]_0[\mathbf{1i}]_{ss}}{K_{m2}} \qquad (6)$$

Note that the second-order rate constant for the initial loss of **1a** of $k_2/K_{m1} = 1.0$ M^{-1} h^{-1} is approximately 4-fold smaller than the second-order rate constant for the formation of **1b** of $k_4/K_{m2} = 4.5$ M^{-1} h^{-1}. If the identity of **1i** were the proposed cis,trans isomer (see eq 2),[16,17] the

(20) Alibrandi, G.; Mann, B. E. *J. Chem. Soc., Dalton Trans.* **1994**, 951.

(21) Segel, I. H. *Enzyme Kinetics*; Wiley: New York, 1993; Chapter 2.

(22) Yang, S.-Y.; Schultz, H. *Biochemistry* **1987**, *26*, 5579.

Scheme 2

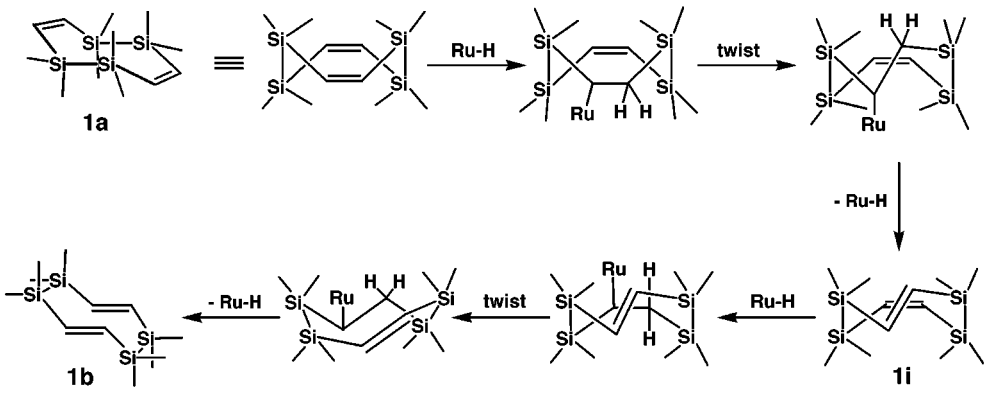

values of the rate constants would indicate that the **Ru** complex is more efficient in isomerizing the cis olefin of **1i** than that of **1a**.

The second-order rate constant for the conversion of **1i** into **1a**, which is indicated by the reverse of eq 3, can be obtained from the slope of a plot of the difference in the initial rate of loss of **1a**, $R_{\mathbf{1a},i}$, and the steady-state loss of **1a**, $R_{\mathbf{1a},ss}$, as a function of $[\mathbf{Ru}]_0$ and $[\mathbf{1i}]_{ss}$ (see Figures S1 and S2 and eqs S4 and S5 in the Supporting Information). The resulting values of the second-order rate constant of $k_{-1}/K_{m-1} = 8.3$ and 6.3 M^{-1} h^{-1} are summarized in Table 2, where $K_{m-1} = (k_2 + k_{-1})/k_{-2}$.

The calculated rate constants can be verified independently. The Haldane relationship[21,22] indicates that the equilibrium constant for a reaction, such as the conversion of **1a** in to **1i** (eq 3), is given by the ratio of the second-order rate constants for the forward reaction to the reverse reaction. Substituting the appropriate second-order rate constants from Table 2 into the Haldane equation predicts an equilibrium constant of $K_{eq} = [\mathbf{1i}]/[\mathbf{1a}] = 0.14$. Semiempirical calculations of the free energy difference between **1a** and the proposed cis,trans intermediate afford an equilibrium constant of 0.04.[16] If **1i** is in fact the cis,trans intermediate as suggested by the preceding studies,[16,17] then there is reasonable agreement between the equilibrium constant calculated from the kinetic data and from the theoretical treatment.

The internal consistency of the kinetic approach can be further tested by defining secondary relationships between observed values. For example, manipulation of the equations here and in the Supporting Information predicts that a plot of the observed $[\mathbf{1i}]_{ss}$ as a function of $[\mathbf{1a}]_0$ will yield a straight line with a slope dependent on the second-order rate constants (see Figure S3 and eq S7 in the Supporting Information). Such a plot was found to be linear with the value of the observed slope equal to 0.089. We note that the corresponding value calculated from the rate constants in Table 2 is equal to 0.084. The agreement between these values demonstrates that our analysis of the kinetics is internally consistent and correctly predicts the steady-state concentration of **1i**. Moreover, it validates the use of the initial rate of loss of **1a** to obtain the value for k_2/K_{m1}, the use of the steady-state rate of formation of **1b** to obtain the value of k_4/K_{m2}, and the difference in the initial and steady-state rates of loss of **1a** as a measure of the value of k_{-1}/K_{m-1}.

Summary of the Kinetics Results. The experimental facts gleaned from the kinetics studies can be summarized as follows:

(1) The **Ru** complex promotes the conversion of the cis,-cis isomer **1a** into the trans,trans isomer **1b** and another component, designated as intermediate **1i**. Both reactions are first order in [**1a**] and in [**Ru**].

(2) The loss of **1a** is accompanied by a lag in the formation of **1b** and the concomitant formation of **1i**, indicating that **1a** is initially converted into **1i**. The intermediate **1i** lies on the pathway for the conversion of **1a** into **1b**.

(3) The second-order rate constant for the initial loss of **1a** of $k_2/K_{m1} = 1.0$ M^{-1} h^{-1} is approximately four times smaller than the second-order rate constant for the steady state formation of **1b** of $k_4/K_{m2} = 4.5$ M^{-1} h^{-1}. If **1i** is in fact the cis,trans isomer, the values of the rate constants indicate that the **Ru** complex is more efficient in isomerizing the cis olefin of **1i** than that of **1a**.

(4) The observed level of $[\mathbf{1i}]_{ss}$ is insensitive to the amount of **Ru**, confirming that the ruthenium complex is involved in both the conversion of **1a** into **1i** and the conversion of **1i** into **1b**.

(5) The agreement for the observed parameters of the figures with predicted values demonstrates the internal consistency of the kinetics methods used. It verifies the use of the initial rate of loss of **1a** to obtain the value for k_2/K_{m1}, the use of the steady-state rate of formation of **1b** to obtain the value of k_4/K_{m2}, and the difference in the initial and steady-state rates of loss of **1a** as a measure of the value of k_{-1}/K_{m-1}.

(6) The second-order rate constants predict a value of 0.14 for the equilibrium constant for the ratio of [**1i**]/[**1a**]. A theoretical calculation predicts an equilibrium constant of 0.04.[16] The agreement in the values supports the identity of **1i** as the cis,trans isomer.

Mechanism of the Isomerization of 1a to 1b. Consistent with known transition metal catalyzed cis−trans olefin isomerization reactions,[3,8] we propose that the **Ru**-promoted isomerization of **1a** to **1b** proceeds via mechanism(s) involving metal hydride addition−elimination. While the origin of the metal hydride in this reaction remains obscure, it is possible that **Ru** or one of its derivatives[14,15] reacts with trace amounts of acid in CD_2Cl_2 to generate a ruthenium hydride. Furthermore, the data in Figure 2 show that the rate of isomerization of **1a** to **1b** increases when the catalyst is preincubated in solvent, consistent with solvent-dependent activation of the catalyst.

The ruthenium hydride addition−elimination mechanism of the isomerization of **1a** is proposed in Scheme 2, explicitly including the cis,trans isomer as intermediate

1i. In this mechanism, **1a** coordinates to a kinetically long-lived ruthenium hydride catalyst and subsequently inserts into the ruthenium-hydride bond to yield a ruthenium alkyl. The ruthenium alkyl twists from a pro-cis configuration to a pro-trans configuration. Subsequent β-elimination yields **1i** and regenerates the ruthenium hydride. Repetition of this process on the remaining cis double bond of **1a** yields **1b** and regenerates the ruthenium hydride.

Although we have been unable to isolate and characterize the proposed cis,trans species **1i**,[23] the results of the kinetics studies are consistent with its proposed intermediacy in the isomerization of **1a** to **1b**. Furthermore, no results were inconsistent with its participation. The loss of **1a** is accompanied by a lag in the formation of **1b** and the concomitant formation of **1i**, indicating that **1a** is initially converted into **1i** and that **1i** lies on the pathway for the conversion of **1a** into **1b.** The second-order rate constants for the conversion of **1a** into **1i** is about four times smaller than that for the conversion of **1i** into **1b**, consistent with a Hammond effect and the predicted instability of **1i** relative to **1b**.[16,17] The measured second-order rate constants can be used to predict an equilibrium constant for [**1i**]/[**1b**] of 0.14, which is consistent with the value of 0.04 derived from semiempirical calculations.[16] Also, spectroscopic data, such as the 600 MHz ^{1}H NMR COSY spectra of the intermediate (data not shown), support the identity of **1i** as the cis,-trans intermediate.

Conclusions

The kinetics of the **Ru**-promoted isomerization of **1a** to **1b** were investigated. Incubation of **Ru** in CD_2Cl_2 for 5 days at 40 °C afforded an active ruthenium hydride catalyst. Exposure of **1a** to the catalytic mixture induced the isomerization, which was observed to proceed in two steps: isomerization of **1a** to intermediate **1i** and subsequent isomerization of **1i** to **1b**. Kinetic studies demonstrated that the two steps were first order with respect to the concentrations of **1a**, **1i**, and **Ru**. The data were further consistent with the occurrence of bimolecular hydride addition−elimination during the two isomerization steps. All data were consistent with a proposed cis,-trans structure for intermediate **1i**.

Experimental Section

Materials and General Methods. The complex (PCy_3)-$RuCl_2$(=CHPh)Ru(*p*-cymene)Cl_2[11] and the compounds 1,1,2,2,5,5,6,6-octamethyl-1,2,5,6-tetrasilacycloocta-3,7-diyne[24] and 1,1,2,2,5,5,6,6-octamethyl-1,2,5,6-tetrasilacycloocta-3,7-diene[16,17] were synthesized according to the indicated literature procedures. The NMR solvent CD_2Cl_2 was purchased from Cambridge Isotope Laboratories. All preincubations and isomerizations were conducted under argon or nitrogen using standard Schlenk line and drybox techniques under ambient laboratory light. ^{1}H NMR spectra were recorded on either a General Electric QE-300 (300 MHz ^{1}H; 75.5 MHz ^{13}C) or a Bruker AMX-II 600 (600 MHz ^{1}H; 151 MHz ^{13}C) spectrometer. All spectra were referenced to an internal solvent resonance (CD_2Cl_2: ^{1}H NMR δ 5.32 ppm; ^{13}C NMR δ 54.00 ppm).

Preincubation of Ru. Three separate Kontes air-free NMR tubes were charged with 0.0037 g (0.0088 mmol) of **Ru** and 0.5 mL of CD_2Cl_2. The solutions were incubated at 40 °C for 0, 5, and 10 days prior to the addition of **1a**. Aliquots of **1a** (0.050 g, 0.35 mmol) and ferrocene (0.0050 g, 0.027 mmol as an internal standard) were then added to each NMR tube. The reactions were allowed to proceed at 40 °C and were monitored by examining the integrals of the olefinic resonances at δ 6.90 of **1a** and δ 6.32 of **1b** relative to the integral of ferrocene.

Kinetics of Isomerization. Seven separate Kontes air-free NMR tubes were charged with the aliquots of **Ru** outlined in Table 1. To each tube was added 0.5 mL of CD_2Cl_2, and the solutions were incubated at 40 °C for 5 days. The aliquots of **1a** outlined in Table 2 along with 0.0050 g (0.027 mmol) of ferrocene as an internal standard were added to each NMR tube. The reactions were allowed to proceed at 40 °C and were monitored by examining the integrals of the olefinic resonances of **1a**, **1i**, and **1b** relative to the integral of ferrocene as described below.

Integration of 1a, 1i, and 1b. During the initial phase of the isomerization (Figure 1), the integral over δ 6.75−6.85 contains olefinic resonance of **1i** (δ 6.78, 2 H). The integral over δ 6.85−7.05 contains the other small olefinic resonance of **1i** (δ 6.88, 2 H) and the olefinic resonance of **1a** (δ 6.90, 4 H). The other small peaks at δ 6.94 and 6.98 in Figure 1 were absent in the initial phase but appeared subsequently. The ratio of the areas of the small peaks at δ 6.78 and 6.88 was 1:1; this ratio was constant over the course of the isomerization. To enhance the accuracy of the measurements, the concentration of **1i** was calculated by simply doubling the integral of the resonance at δ 6.78. Furthermore, the integral of the resonance at δ 6.78 was subtracted from the integral over δ 6.85−7.05 to give the concentration of **1a** during the initial phase. During the steady-state phase of the isomerization, the concentration of **1i** was again calculated by simply doubling the integral of the resonance at δ 6.78. However, the integration of **1a** was complicated by presence of two additional small peaks at δ 6.94 and 6.98, which were tentatively assigned to decomposed catalyst (vide supra). Since the ratio of all four small resonances was roughly 1:1 during the steady-state phase (e.g., Figure 1), we calculated the integral of **1a** by subtracting three times the integral of the small resonance at δ 6.78 from the integral over δ 6.85−7.05. The integral of olefinic resonance for **1b** (4 H) was collected over δ 6.05−6.45 to include the broad shoulder, which arises from the presence of equilibrium conformers.[17]

Integration of the Internal Standard. The integral (δ 4.5−3.8) of the peak for the internal standard ferrocene (δ = 4.18 ppm) was arbitrarily set to a maximum value of 100; all other integrals were calculated relative to the internal standard.

Measurement of Initial and Steady-State Rates. The values of $R_{\mathbf{1i},\mathrm{i}}$ were measured as the slopes of the lines tangent to the initial phase of the formation of **1i**. The values of $R_{\mathbf{1a},\mathrm{i}}$ were calculated on the basis of $R_{\mathbf{1i},\mathrm{i}}$. The values of $R_{\mathbf{1a},\mathrm{ss}}$ and $R_{\mathbf{1b},\mathrm{ss}}$ were measured as the slopes of the progress curves in the steady-state region as a function of the total concentration of **1a** (see Figures 4 and 5).

Acknowledgment. We thank the National Science Foundation (CAREER Award to T.R.L.; CHE-9625003), the Texas Advanced Research Program (Grant No. 003652-162), and the Robert A. Welch Foundation (Grant No. E-1320) for generous financial support. We are also grateful to Dr. Adrian Whitty (Biogen) for many helpful discussions.

Supporting Information Available: Description and derivation of equations 5, 6, and S1−S8; description and graphic presentation of Figures S1−S3. This material is available free of charge via the Internet at http://pubs.acs.org.

JO0014820

(23) Attempts to isolate the intermediate **1i** by chromatographic methods (including preparative TLC) were unsuccessful.

(24) Iwahara, T.; West, R. *J. Chem. Soc., Chem. Commun.* **1988**, 954.